

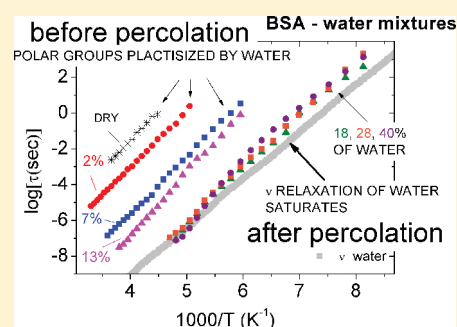
Protein and Water Dynamics in Bovine Serum Albumin–Water Mixtures over Wide Ranges of Composition

A. Panagopoulou,^{*,†} A. Kyritsis,[†] N. Shinyashiki,[‡] and P. Pissis[†]

[†]Department of Physics, National Technical University of Athens, Zografou Campus, 157 80 Athens, Greece

[‡]Department of Physics, Tokai University, Hiratsuka, Kanagawa, 259-1292 Japan

ABSTRACT: Dielectric dynamic behavior of bovine serum albumin (BSA)–water mixtures over wide ranges of water fractions, from dry protein until 40 wt % in water, was studied through dielectric relaxation spectroscopy (DRS). The α relaxation associated with the glass transition of the hydrated system was identified. The evolution of the low temperature dielectric relaxation of small polar groups of the protein surface with hydration level results in the enhancement of dielectric response and the decrease of relaxation times, until a critical water fraction, which corresponds to the percolation threshold for protonic conductivity. For water fractions higher than the critical one, the position of the secondary ν relaxation of water saturates in the Arrhenius diagram, while contributions originating from water molecules in excess (uncrystallized water or ice) follow separate relaxation modes slower than the ν relaxation.



1. INTRODUCTION

It is known that the dynamics of water is experimentally inaccessible for the liquid state in a wide temperature range (150–230 K at atmospheric pressure), often called the no man's land. This is due to the fact that, even after quenching to very low temperatures, bulk supercooled water crystallizes upon heating at approximately 150 K.¹ In order to confront the difficulty in monitoring water dynamics in the no man's land region, several approaches have been made in the literature, aiming to prevent crystallization of water, either by mixing with hydrophilic glass-forming solutes^{2–6} and biopolymers^{7,8} or by confinement on the nanometer length scale,^{9–13} e.g., within nanopores of silica gels.⁹ Homogeneous water solutions of several systems, such as alcohols, ethylene and propylene glycols, sugars, or carbohydrates (mono-, di-, and polysaccharides), and some hydrophilic macromolecular systems including biopolymers (from polypeptides to several proteins),^{3,4,14,15} in concentrations of water up to 50% in weight, can be easily supercooled down to form glass, while no crystallization occurs when water molecular clusters are reduced down to sizes smaller than the critical size necessary for homogeneous nucleation, in case of confinement.⁹ Another effect of confinement is the disorder induced by the interfaces that prevents the water molecules from forming a crystalline lattice.

Dielectric studies focused on the dynamics of supercooled water in different host environments in the hydration range 30–50 wt %, all providing one major result concerning the main relaxation of water. Its relaxation time, τ , has an Arrhenius temperature dependence, at least below the glass transition temperature, T_g , of the hydrated system, has an almost universal activation energy, E_{act} , of about 0.45–0.55 eV,^{4,16} and shows a symmetric or nearly symmetric shape of its response function on a logarithmic frequency scale, and its magnitude increases

systematically with increasing water content.¹⁶ These characteristics apply not only in the case of aqueous mixtures but also in the case of water confined in various confining systems.¹⁷ Another interesting feature of the observed main relaxation is a change in the temperature dependence of its characteristic relaxation time from an Arrhenius to a non-Arrhenius one (strong to fragile crossover), typically at about 180 ± 20 K.^{4,14,18} In the case of hydrated proteins, this dynamic crossover has been assigned to the saturation of the cooperative ordering of hydrogen bonds, by combining experimental results and molecular simulations.¹⁹ However, several experimental studies on hydrated proteins by dielectric relaxation spectroscopy (DRS) and nuclear magnetic resonance (NMR) show no sign of such a crossover,^{20,21} which has also been suggested to be an artifact of the data analysis method.²² More recent studies propose the presence of more than one dynamical crossover, one at about 250 K and one at about 180 K, for protein hydration water.²³ The crossover at about 180 K has been also observed in the case of protein hydration water and water confined in silica gel nanopores.²⁴

The interpretation of the main relaxation of water and its association to the viscosity related α relaxation of bulk water has been highly debated in the literature. Unlike simple liquids, there is a difficulty to extrapolate the time scales of the dielectric response of water above the homogeneous nucleation temperature (235 K) to the one in the deeply supercooled regime. The T_g of water is suggested to be in the range of 136 K,^{25–28} while other studies suggest that the actual glass transition temperature of water lies in the range 160–180

Received: November 3, 2011

Revised: March 7, 2012

Published: April 2, 2012



K.^{9,29–32} The dynamic crossover of the main relaxation of water has been interpreted to originate from a transformation of a secondary β relaxation of water in the deeply supercooled regime into a cooperative viscosity related α relaxation above the crossover temperature^{3,4,33} or in the fact that, at temperatures above the crossover temperature, a merged $\alpha\beta$ relaxation is observed, while the α relaxation disappears at lower temperatures due to confinement effects.¹⁸ On the other hand, the nature of the corresponding relaxation has been discussed in terms of the Johari–Goldstein β relaxation of glass formers in general in refs 14, 15, and 34–36 where the term “ ν relaxation” of water was used. In refs 34 and 36, the ν relaxation of water is strongly believed to have exclusive characteristics like a secondary relaxation process, as its dielectric strength $\Delta\epsilon$ universally increases with temperature, unlike in the case of a viscosity related α relaxation. Additionally, it was shown by numerous experimental results on different systems that the time scale of the ν relaxation process depends on the hydration level and a bottom limit for this was suggested.³⁶

In the case of hydrated proteins, the main relaxation of water is usually attributed to contributions of water molecules in the protein hydration shell.^{37–41} Although most dielectric spectroscopy studies are dealing with samples of hydration levels high enough for complete hydration and low enough to prevent crystallization of water (about 30 wt %), recently efforts were made to study protein dynamics in a broad hydration range, either in partially crystallized solutions⁸ or starting at low levels of hydration with hydrated dry samples (powders).^{20,21,42–44} Studies at low levels of hydration have been able to follow the secondary relaxation of water and to establish an additional contribution from the protein surface itself to the dielectric response.^{20,43,44} Dielectric studies using insulating thin foils in the case of hydrated myoglobin⁴² and hydrated glutathione (a model system for protein–water interactions)⁴⁵ revealed a rich dielectric response including contributions due to protein and water. Two recent studies by our group combining differential scanning calorimetry (DSC) and two dielectric techniques, dielectric relaxation spectroscopy (DRS) and thermally stimulated depolarization currents (TSDC), but also equilibrium sorption isotherm (ESI) measurements at room temperature, in extremely broad ranges of hydration levels, for two globular hydrated proteins, lysozyme⁴³ and bovine serum albumin (BSA),⁴⁴ have provided new results regarding the protein glass transition, as well as the reorganization of distinct water populations in the uncrystallized or crystallized phase, interfering in several processes.

In this work, DRS data of hydrated BSA at wide ranges of hydration levels and broad frequency and temperature range, both solutions and solid pellets, are being analyzed by fitting model functions to the data, aiming at a detailed study of dynamics of water in the mixtures. The results are discussed in relation to the results in ref 44 and to other results on water containing systems appearing in the literature. The combination of different experimental techniques at wide ranges of water content has proven to provide remarkable consistency of results in the case of hydrated proteins and other water containing biological systems,^{43,44,46} although this kind of experimental approach is rather rare.

2. EXPERIMENTAL METHODS

2.1. Sample Preparation. Albumin from bovine serum (BSA) in the form of lyophilized powder (Sigma 3294) was purchased from Sigma-Aldrich (Mr~66.000) and used as

received. Water with 10 $\mu\text{S}/\text{cm}$ conductivity was employed for preparation of the samples. Samples for dielectric (DRS) measurements were either in the form of solutions (for water fraction 40 wt %) or in the form of solid compressed pellets (for low water fractions, lower than 40 wt %). The diameter of the pellets was 12 mm and their thickness about 1 mm. The dry sample was obtained by drying in an oven under a vacuum at 333 K for 72 h. For preparing the solution, BSA was dissolved in water, and for homogenization of the sample, the mixture was kept at 277 K for at least 2 days before the measurement. Solid samples were hydrated to the required degree by equilibration for more than 3 days (to constant weight) above saturated salt solutions in sealed jars. The samples were kept in sealed plastic bags within sealed jars, in 100% relative humidity, for an additional period of more than 10 days, in order for the adsorbed water molecules to be homogeneously distributed. The water fraction of the samples is expressed on the wet basis, i.e., (grams of water per grams of hydrated protein) \times 100%.

2.2. Dielectric Relaxation Spectroscopy Measurements. For DRS measurements,⁴⁷ the complex dielectric function (known also as dielectric permittivity and dielectric constant), $\epsilon^*(f) = \epsilon'(f) - i\epsilon''(f)$, was determined as a function of frequency, f (10^{-1} – 10^6 Hz), at constant temperature (123–273 K, controlled to better than ± 0.1 K), using a Novocontrol Alpha Analyzer in combination with a Novocontrol Quatro Cryosystem. For measurements, the solid samples were placed between two electrodes forming a cylindrical capacitor 12 mm in diameter. The solution was placed between electrodes 20 mm in diameter kept apart by silica spacers 50 μm in thickness. Our electrode configurations include no insulating electrodes aiming at recording the net dielectric response of the system under study.

2.3. Data Analysis. The contribution to the complex permittivity from each relaxation, j , was modeled by an empirical Cole–Cole function:⁴⁸

$$\epsilon_j^*(f, T) = \frac{\Delta\epsilon_j(T)}{1 + (2\pi if\tau_j(T))^{\beta_j(T)}} \quad (1)$$

where $\Delta\epsilon_j(T)$, $\tau_j(T)$, and $\beta_j(T)$ are the dielectric strength, relaxation time, and fractional exponent of process j , and the contribution of the direct current (dc) to the imaginary part of the complex permittivity by a conductivity term: $\epsilon''(f) = \sigma(T)/\epsilon_0(2\pi f)$, where σ is the dc conductivity and ϵ_0 the permittivity of free space.

3. RESULTS

Dielectric measurements were performed for BSA–water mixtures with water fractions of 0, 2, 7, 18, 28, and 40 wt %. All samples were in the form of compressed pellets, except for the one with 40% in water, which was in the form of concentrated solution. The issue about comparing hydrated powders and solutions, in terms of hydration properties and water organization, should be highlighted at this point. As it will be shown in the following, the current results show significant consistency, as the samples of 28 and 40% water fraction (hydrated powder and solution, respectively) exhibit similar relaxation modes. These results support similar findings in previous works of our group (refs 43 and 44) where it was shown that the results obtained on a broad range of hydrated pellet samples and solutions are consistent with each other.

3.1. Raw Data. Figure 1 shows dielectric loss versus frequency, $\epsilon''(f)$, isothermal data, for the dry BSA pellet, at

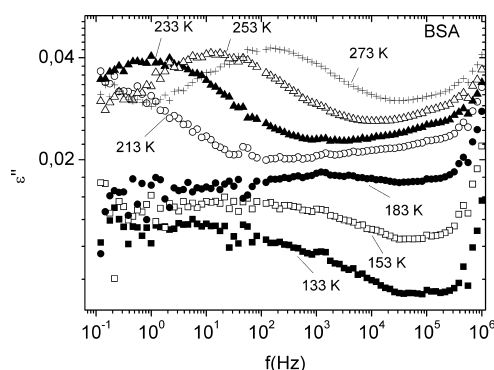


Figure 1. Dielectric loss versus frequency, $\epsilon''(f)$, for a dry BSA sample at selected temperatures T indicated on the plot.

selected temperatures indicated on the plot. As it can be seen, the dielectric response is very low for this sample, and we present it separately, so that information is not eliminated due to scaling, when represented in comparative diagrams with the rest of the hydrated samples. Two relaxation processes can be detected within the experimental temperature range. At low temperatures, a broad peak enters the experimental window, centered at about 0.5 and 1 kHz at 133 and 183 K, respectively. At higher temperatures, a symmetric peak enters the experimental window at 213 K, centered at about 1, 20, and 200 Hz at 233, 253, and 273 K, respectively. The origin of the two relaxations in question will be discussed in the Discussion section of this paper.

The frequency dependence of the real and imaginary part of the dielectric function, ϵ^* , measured at $T = 258$ K is shown in Figure 2, for several samples of different hydration levels. At this temperature, a relaxation peak (α relaxation), which will be shown that it is associated with the glass transition of the hydrated protein,⁴⁴ is within the experimental window for most of the samples, as is indicated by the main step in the $\epsilon'(f)$ plots (Figure 2a) and the low frequency peak in the $\epsilon''(f)$ plots (Figure 2b). Looking at the dielectric loss curves in Figure 2b, we observe that the α relaxation peak is absent for the sample of water fraction 2%. The low intensity peak which is within the experimental window, centered at about 800 Hz for the sample of water fraction 2%, corresponds to a relaxation of small polar groups of the protein triggered by water, as will be shown later. For water fraction 7%, the maximum of the α peak is not observable and is probably located at lower frequencies (measurements at higher temperatures reveal the existence of the α relaxation peak). The α peak is observable in Figure 2b for water fraction 13% as a shoulder, while its maximum is clearly visible for water fraction 18%. Although the conductivity contribution is large at this relatively high temperature, rough estimations of the peak position (based also on the corresponding $\epsilon'(f)$ plots) are highlighted in Figure 2b by arrows.

Dielectric permittivity versus frequency, $\epsilon'(f)$, and dielectric loss versus frequency, $\epsilon''(f)$, isothermal data at temperature $T = 183$ K are plotted in Figure 3a and b, respectively, for several samples of different hydration levels. In Figure 3a, we observe that the measured dielectric permittivity increases with increasing water fraction, in the whole frequency range measured, up to a water fraction of 28%, whereas for 40% it

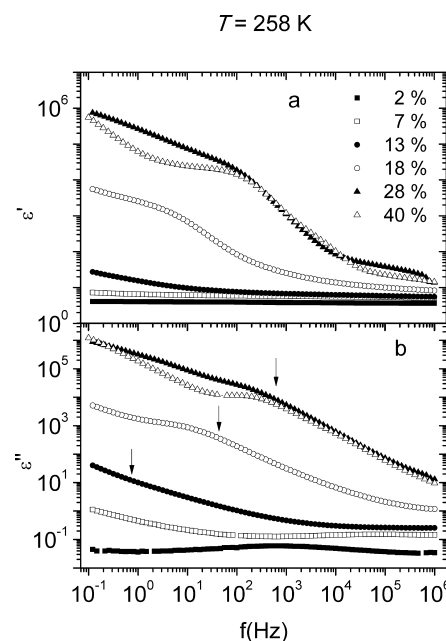


Figure 2. (a) Real part of the dielectric function against frequency, $\epsilon'(f)$, and (b) imaginary part of dielectric function (dielectric loss) against frequency, $\epsilon''(f)$, at 258 K, for BSA–water mixtures at several water fractions indicated on the plot. The arrows indicate rough estimations of the overall α relaxation peak maximum.

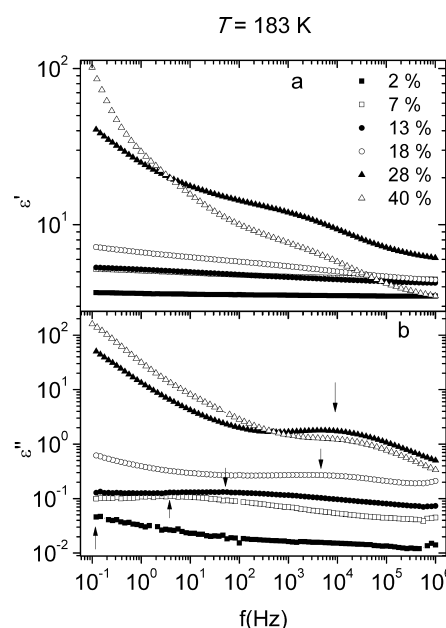


Figure 3. (a) Real part of the dielectric function against frequency, $\epsilon'(f)$, and (b) dielectric loss against frequency, $\epsilon''(f)$, at 183 K, for BSA mixtures at several water fractions indicated on the plot. The arrows indicate the estimated peak maximum.

drops to lower values at the high frequency part of the spectrum. In addition, the $\epsilon'(f)$ plots show that for water fractions higher than 18% the dielectric permittivity increases remarkably at low frequencies, implying the activation of strong polarization processes at that water fraction range. Dielectric loss spectra shown in Figure 3b reveal the existence of a relaxation process which depends strongly on the hydration level. More specifically, the sample of water fraction 2% exhibits a relaxation peak at the low frequency side of the experimental

window, the maximum of which is not clearly detectable, as it is probably located at lower frequencies. For the sample of 7% in water, a broad relaxation peak is observed centered at about 30 Hz. This peak corresponds to a relaxation of small polar groups of the protein which is triggered by water in the hydration shell (as has been discussed in ref 44), and is shifted with respect to the peak for the sample of 2% in water (plasticized by water). The plasticization of the underlying molecular process for higher water fractions can be followed in Figure 3b. Arrows in the diagram indicate the maximum frequency of the peak, which is at about 500 Hz for 13% and 50 kHz for 18%. The position and the magnitude of the peak seem to saturate for samples of 28 and 40% in water, centered at about 10 kHz. At this point, we would like to highlight the increase of the measured low frequency dielectric loss for water fractions higher than 18%. Taking into consideration also the remarkable increase of $\epsilon''(f)$ at that water fraction and frequency range, we may conclude that the conductivity of the samples is significantly enhanced for that water fraction range, implying that the conduction process becomes now a percolative type process.⁴⁹

3.2. Fitting Results. Dielectric data corresponding to the samples of hydration levels lower than 18% have been expressed as the sum of two or three Cole–Cole functions and a conductivity term, at temperatures where this was necessary. The two samples of lowest hydration levels (0 and 2%) exhibit two secondary relaxations and no α relaxation associated with the glass transition of the protein. The peaks of these relaxations are clearly visible for the dry sample and have been presented in Figure 1. The high temperature peak originates from the movement of small polar groups of the protein surface, while the low temperature peak will be further analyzed later on. The data corresponding to the samples with water fractions 7, 13, and 18% exhibit, except from the relaxation of polar groups, a peak corresponding to the α relaxation associated with the glass transition of the hydrated system.

Fitting of the dielectric loss curves for the samples of higher water fractions, that is, 28 and 40%, has revealed additional peaks entering the experimental window, originating possibly from new forms of water organization (excess water or ice), as the water fraction increases. The complexity of the dielectric response (multiple interfering peaks) along with the large conductivity contribution at high water fractions make the detection of the peaks rather tentative, in contrast to lower water fractions where the curves are more simple. Help may often be provided by using a derivative method:⁵⁰

$$\epsilon''_{\text{der}}(f) = -\frac{\pi}{2} \frac{\partial \epsilon'(f)}{\partial \ln f} \approx \epsilon''_{\text{rel}} \quad (2)$$

where ϵ''_{rel} is the ohmic-conduction-free dielectric loss, provided that conductivity makes no significant contribution to ϵ' . For that reason, the dielectric loss calculated by the derivative method is added to diagrams containing fitting of dielectric loss at high water fractions.

An example of the fitting of the dielectric loss curves for the samples of water fractions 7, 18, and 28% (inset) and 40%, at a characteristic temperature of 183 K, where the relaxation of polar groups and the ν relaxation of water is within the experimental window, is shown in Figure 4. Starting with the data corresponding to the sample of 7% water fraction, a broad peak corresponding to a relaxation of polar groups of the

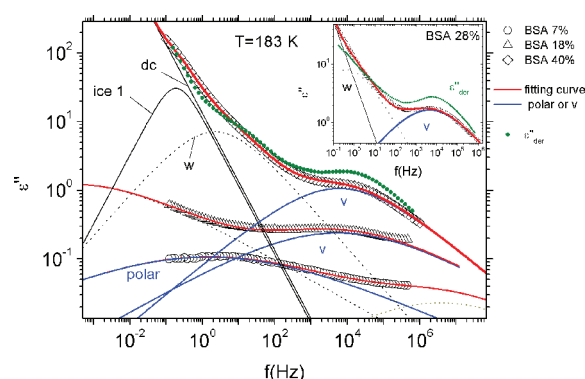


Figure 4. Dielectric loss against frequency, $\epsilon''(f)$, at 183 K, for BSA–water mixtures of water fractions 7, 18, and 28 (inset) and a BSA–water solution of water fraction 40%. The green solid circles correspond to dielectric loss calculated by the derivative method.⁵⁰ The blue solid lines show the peaks corresponding to the relaxation of polar groups for the 7% sample and the ν relaxation of water for the rest of the samples. The solid red lines through the experimental data correspond to the sum of the contributions.

protein can be seen centered at about 1 Hz. A peak at higher frequencies (dotted line) is necessary to fit the data, but it is not dealt with in this article, as its maximum is located mainly out of the frequency range of the experimental window. The same applies for other such peaks in the fitting procedure. At higher water fractions, that is, 18, 28 (inset), and 40%, a peak corresponding to the ν relaxation of water can be seen centered at about 10^4 Hz. The ν peak³⁴ seems to be related with the reorientation of the water molecules at the protein surface. The interplay of this relaxation with the local relaxation of small polar groups of the protein surface triggered by water at lower hydration levels will be discussed later on. An additional peak named w , centered at about 1 Hz for the samples of water fractions 28 and 40%, is presented as a dotted line, because its maximum could not be clearly discerned at any temperature of our measurements. Its existence is alternatively verified indirectly, e.g., by the change of slope of the dielectric loss, which is more pronounced in the derivative data (sample of 40% water fraction, green circles) and of course by the fact that fitting was not possible without taking process w into account. For that reason, we assumed a value of $\beta_w = 0.6$ for the fractional exponent of process w , which was set as a constant during the fitting procedure. Finally, a peak, better fitted as Debye (i.e., $\beta = 1$ in eq 1), signed as $ice1$ is centered at about 0.1 Hz, in the case of the sample of 40% water fraction.

Figures 5 and 6 are examples of the fittings at selected temperatures, 238 and 168 K, respectively, for the sample of 40%. Figure 5 shows the peaks contributing to dielectric spectra at a high temperature, $T = 238$ K, for BSA 40%. Starting at low frequencies, a Debye peak named p on the plot is hidden below the dc conductivity contribution. The maximum of this peak is clearly visible at higher temperatures, and the peak is necessary to fit the data, but it will not be further studied in this paper, so it is plotted as a dotted line. Similar dielectric responses are often encountered in dielectric measurements on water containing systems and are usually interpreted as interfacial polarization processes due either to localized conduction processes within the samples or to electrode polarization effects.^{8,51,52} In addition, such a relaxation process is usually modeled by a Debye relaxation process.⁵³ Analogous peaks were used for fitting the data of water fractions higher than 7%.

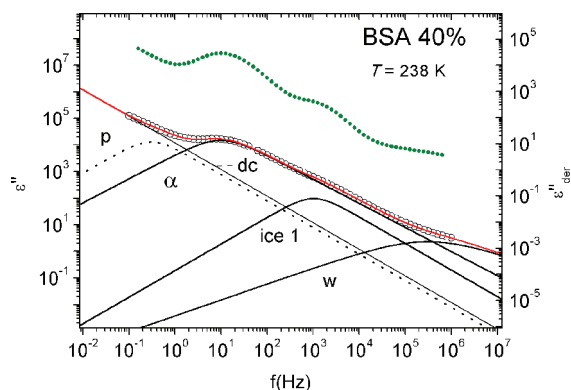


Figure 5. Dielectric loss against frequency (open circles), $\epsilon''(f)$, at 238 K, for a BSA–water solution of water fraction 40%. Green solid circles correspond to dielectric loss data calculated by the derivative method.⁵⁰ Solid and dotted lines correspond to contributions to dielectric loss calculated by fitting of the data by a sum of Cole–Cole functions and a conductivity term. The solid line through experimental data (open circles) corresponds to the sum of the contributions.

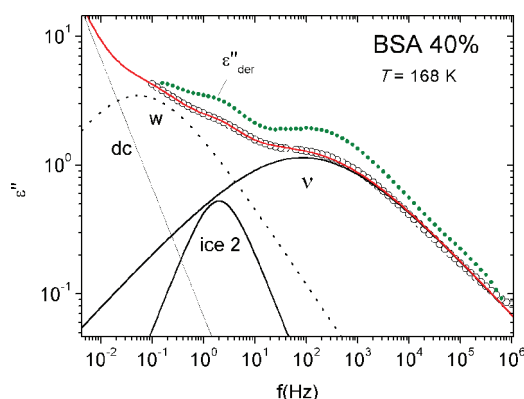


Figure 6. Dielectric loss against frequency (open circles), $\epsilon''(f)$, at 168 K, for a BSA–water solution of 40% water fraction. Green solid circles correspond to dielectric loss data calculated by the derivative method.⁵⁰ Solid and dotted lines correspond to contributions to dielectric loss calculated by fitting of the data by a sum of Cole–Cole functions and a conductivity term. The solid line through experimental data (open circles) corresponds to the sum of the contributions.

At higher frequencies in Figure 5, additional peaks follow, namely, the α peak associated with the glass transition of the hydrated protein, centered at about 10 Hz, a Debye peak probably due to ice, signed as *ice1*, centered at about 1 kHz, and a peak signed as *w* (which has been discussed above, Figure 4). The position of the peaks seems to correlate well with that calculated by the derivative method (open triangles). Moving on to lower temperatures ($T = 168$ K, Figure 6), a Debye process signed as *ice2* is observable (in addition to the ν and the *w* peak), centered at about 2 Hz at 168 K. The peaks denoted as *ice1* in Figure 5 and *ice2* in Figure 6 are attributed to relaxation processes in the ice phase, because they were detected only for the sample of 40%, where ice crystals have been formed during cooling,⁴⁴ while they were absent in the case of the 28% sample, where DSC studies show no ice formation during cooling.⁴⁴

The fitting parameters $\tau_j(T)$ (relaxation time) and $\Delta\epsilon_j(T)$ (dielectric strength) calculated for each process j are plotted in Figures 7–10 against temperature, while the parameters $\beta(T)$ for the processes of polar groups of the protein triggered by

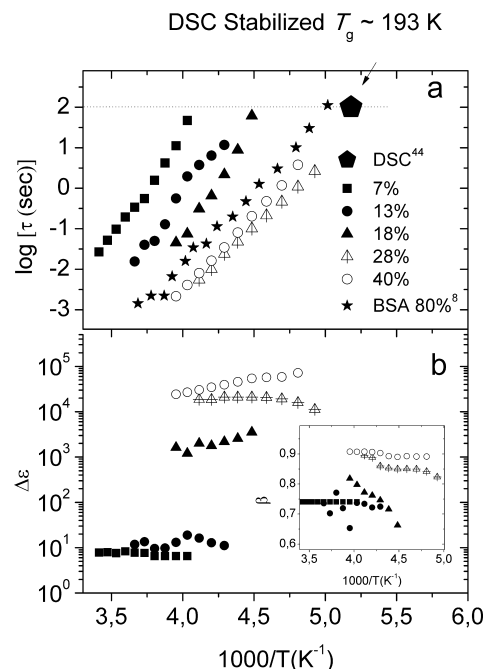


Figure 7. (a) Temperature dependence of the relaxation times for the α relaxation associated with the glass transition of the hydrated BSA, for samples of different water fractions indicated on the plot. Solid stars are data from ref 8 on a BSA–water solution of 80% water fraction. (b) Relaxation strength $\Delta\epsilon_\alpha$ of the α relaxation associated with the glass transition of the hydrated BSA, for samples of different water fractions indicated on the plot. The inset shows the fractional exponent $\beta(T)$ of the Cole–Cole functions of the α relaxation peaks.

water, at low hydration levels, and for the ν relaxation of water associated with the main relaxation of water at high hydration levels, are listed in Table 1. The data of Figure 8 for the

Table 1. Fractional Exponent $\beta(T)$ of the Cole–Cole Function for the Process of Polar Groups–Hydration Water for the BSA Samples of Hydration 0–13 wt % and for the ν Relaxation of Water for Samples in the Hydration Range 18–40%

water (wt %)	0	2	7	13	18	28	40
$\beta(T)$	0.38	0.32	0.23	0.15	0.30	0.43	0.43

relaxation of polar groups of the protein triggered by water (high temperature relaxation peak in Figure 1 concerning the dry sample and relaxation peaks in Figure 3b) and the ν relaxation of water (relaxation peaks in Figure 3b) have been expressed by an Arrhenius equation, $f = f_0 \cdot e^{-(E_{\text{act}}/kT)}$, where E_{act} and f_0 are the activation energy and the pre-exponential factor, respectively. The corresponding values of the activation energy E_{act} as well as the logarithm of the pre-exponential factor $\log f_0$ are listed in Table 2.

4. DISCUSSION

4.1. α Relaxation of the Hydrated Protein. In a recent study by DSC on a BSA–water system over wide ranges of water fraction,⁴⁴ a broad and weak heat capacity step has been observed for water fractions higher than about 7% (in particular, for water fractions equal to or higher than 10%), and this can be seen in Figure 3 of ref 44. The T_g value was found to decrease significantly with addition of water and to

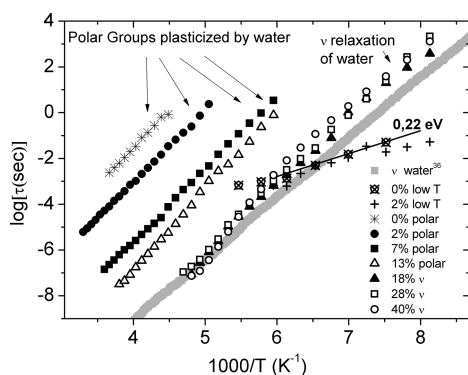


Figure 8. Temperature dependence of the relaxation times for (i) the low temperature relaxation in dry BSA and BSA 2% in water, (ii) a relaxation of small polar groups of the protein surface triggered by water for BSA–water mixtures of water fractions 0, 2, 7 and 13%, and (iii) the ν relaxation of water for hydrated BSA pellets of water fractions 18 and 28% and a BSA–water solution of water fraction 40%.

Table 2. Activation Energy, E_{act} , and Logarithm of the Pre-Exponential Factor, $\log f_0$, of the Arrhenius Equation for the Relaxations of Small Polar Groups of BSA Which Is Triggered by Hydration Water (0–13%) and for the ν Relaxation of Water (18, 28, and 40%)^a

water (wt %)	E_{act} (eV)	$\log f_0$
0	0.67 ± 0.01	14.14 ± 0.20
2	0.62 ± 0.01	14.67 ± 0.12
7	0.63 ± 0.01	17.60 ± 0.09
13	0.70 ± 0.01	20.08 ± 0.15
18	0.55 ± 0.02	18.83 ± 0.75
28	0.59 ± 0.01	19.92 ± 0.32
40	0.50 ± 0.01	16.95 ± 0.19

^aThe activation energy of the ν relaxation has been calculated for temperatures lower than the crossover temperature of about 170 K.

stabilize at about 193 K, for water fractions higher than about 30% (see Figure 4 in ref 44). The water fraction value of 30%, where the plasticization of the hydrated protein is ceased, was found to correspond to the onset water fraction for both, the crystallization of water during cooling and the stabilization of the fraction of uncrystallized water (20–25%) which does not crystallize neither during cooling nor heating (as it is calculated by comparing the enthalpy of the recorded melting peak with the melting enthalpy of bulk ice).⁴⁴ Figure 7a and b shows the temperature dependence of the relaxation time for the α relaxation associated with the glass transition of the hydrated BSA and the corresponding dielectric strength $\Delta\epsilon_\omega$ respectively. The inset in Figure 7b shows the fractional exponent $\beta(T)$ of the Cole–Cole functions of the α peaks. In Figure 7a, a strong plasticization of the α relaxation is observed with addition of water, for water fractions 7–28%. Further addition of water causes no further change in the time scale of the α relaxation, as the position of the data for the sample of 40% follows the same trace with that of 28%. This behavior is consistent with the calorimetric results mentioned above.⁴⁴ Additionally, an extrapolation of the data of these two samples to the equivalent relaxation time for calorimetric measurements ($\tau = 100$ s) seems to coincide with the stabilized T_g value from ref 44. Furthermore, data from ref 8 which correspond to the dielectric process III associated with the glass transition of a BSA–water solution 80% (filled stars in Figure 7a) are similar

with our data for 28 and 40%. This value for the T_g of hydrated BSA after stabilization is in the range of the values reported in the literature for the thermal glass transition of various proteins, that is, in the range 163–203 K, depending on the protein, the hydration level, and the experimental technique employed.^{54–58} The prementioned observations provide strong evidence that the data in Figure 7a correspond to the α relaxation. The presentation of the plasticization of the protein α process in an Arrhenius diagram is, to the best of our knowledge, a novel result.

Considering the relaxation strength $\Delta\epsilon_\alpha$ of the α process, it can be seen in Figure 7b that it increases superlinearly with hydration level. Furthermore, a clear increase of $\Delta\epsilon_\alpha$ with temperature decrease (which is typical for the α relaxation of glass forming materials),³⁶ is observed only for the samples of 18 and 40%. Considering the sample of 28% water fraction, this inconsistency can be explained by the fact that this water fraction value is within the water fraction range where cold crystallization effects occur (23% to about 30%).⁴⁴ Cold crystallization of ice in this case could be interfering in the temperature range of the α relaxation affecting the values of the dielectric strength. In the case of the samples of low water fractions, that is, of 7 and 13%, we know that cold crystallization is absent. On the other hand, the low intensity of the α peak at these low water fraction values along with its high relaxation time, when compared with the other samples, result in an increased uncertainty of the fitting results, as conductivity contributions are large in proportion to the magnitude of the peaks. This difficulty in monitoring the α peak is more obvious in the case of the 13% sample, where it can be seen in the inset of Figure 7b that there is significant scattering of the fractional exponent $\beta(T)$. Considering the sample of 7% in particular, we may also highlight the fact that this is a value close to the onset water fraction for the appearance of the protein glass transition and that it was fitted without an additional Debye p peak (see section 3.2), which was needed for the other samples at higher water fractions. The origin of the glass transition in hydrated proteins is anyway highly debated in the literature, and it has been proposed that it is highly connected to water and, particularly, that it leads to the cooperative motion of water in the hydration shell and protein chains.^{8,44,58,59} This fact may be the reason for the peculiarity of the protein glass transition, compared to that of common glass formers. The aim of this paper is not to analyze in detail the dynamics of the α relaxation of the hydrated protein, as conductivity contributions and polarization effects are significant in the temperature region where the α relaxation is observed (we also recall the existence of an additional process p near the α peak). More experiments are needed for such an analysis. On the other hand, the assignment of the processes associated with the protein glass transition provides help for the interpretation of the relaxations originating mainly from water dynamics.

4.2. The Interplay between a Secondary Relaxation of Polar Groups Triggered by Water Molecules and the ν Relaxation of Water. The temperature dependence of the time scale of the secondary relaxation associated with small polar groups of the protein triggered by hydration water (high temperature peak in Figure 1 for the dry sample and peaks in Figure 3b for samples of low hydration, 2, 7, and 13%) and of the ν relaxation of water for samples 18, 28, and 40% (peaks in Figure 3b) is shown in Figure 8. The temperature dependence of relaxation times for the low temperature relaxation of the dry

sample (Figure 1) and the sample of 2% (see "Raw data" section) can also be seen in the Arrhenius diagram of Figure 8. This low temperature relaxation follows an Arrhenius law, and it is characterized by an activation energy, $E_{\text{act}} = 0.22$ eV. This value is very close to the energy required to break a single hydrogen bond, and this probes us to assume that this relaxation is probably associated with the reorientation of water molecules dispersed in the protein, in such a way that they are completely isolated from each other. It is essential to mention that a relaxation of similar E_{act} although faster, has been recorded in the case of lysozyme–water mixtures of high water content studied by NMR²¹ and there it was assigned again to a form of water. Furthermore, its position in the Arrhenius diagram coincides with that of process I_{α} from ref 8 in the case of a BSA–water solution of water fraction 80%, and there it was assigned to uncrystallized water. More experimental studies are essential to clarify the origin of the relaxation in question and its evolution with hydration level.

Moving to the high temperature side of Figure 8, we may follow the relaxation of small polar groups, mentioned previously, plasticized by water, until a water fraction of 13%. The activation energy of this relaxation is in the range 0.6–0.7 eV (Table 2). The interpretation that this relaxation process is assigned to the movement of polar groups rather than water molecules alone is driven first by the observation of this relaxation already for the dry sample and also by its strong plasticization by water, which is very common in the case of secondary relaxations in polymeric materials. The plasticization is stronger for low water fractions, from the dry sample until the sample of 7% in water. It is obvious that the trace of the data is moving to lower temperatures more smoothly for further increase of the water fraction from 7 to 13%. The same applies for the increase of the relaxation strength $\Delta\epsilon$, shown in Figure 9. Similar behavior regarding the plasticization rate against

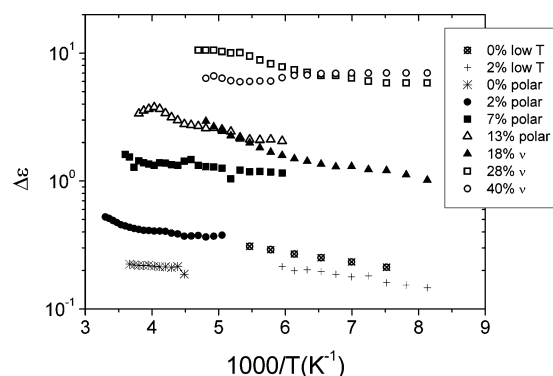


Figure 9. Relaxation strength $\Delta\epsilon$ of (i) the low temperature relaxation in dry BSA and BSA 2% in water, (ii) a relaxation of small polar groups of the protein surface triggered by water for BSA–water mixtures of water fractions 0, 2, 7 and 13%, and (iii) the ν relaxation of water for hydrated BSA pellets of water fractions 18 and 28% and a BSA–water solution of water fraction 40%.

increasing water fraction has been observed in the case of casein⁶⁰ and lysozyme⁴³ by TSDC measurements with systematic variation of the water fraction in small steps. In both cases, a saturation of the peak position was observed at water fraction values comparable with the critical values for the completion of the first hydration layer estimated by ESI. The saturation of the plasticization along with the superlinear increase of $\Delta\epsilon$ at even higher water fractions, which has also

been recorded in the case of hydrated elastin and collagen,²⁰ are in consistency with the conclusions from ref 44, where it was shown that at a water fraction of about 7% the primary sorption sites of the protein surface (first sorption layer, hydrophilic polar groups) is completed, and clustering of the water molecules at the vicinity of the protein surface sets in, resulting in additional contributions of water molecules themselves within the water clusters (ν process). This scenario has been very well described in a review by Careri et al.,⁶¹ in the case of globular proteins. This is also supported by the values of the fractional exponent $\beta(T)$ of the relaxation of polar groups for BSA–water mixtures of 0, 2, 7, and 13% (Table 1), which decreases from a value of 0.38 for the dry sample to 0.15 for 13%. This shows that the distribution of relaxation times becomes broader as water clustering increases, resulting in a less homogeneous sample. At the same time, at the hydration level where water clustering sets in, the additional water molecules, in the form of extended clusters, interact locally with the protein surface, so that segmental movement appears in the system, observed dielectrically for water fraction higher than 7%. At low hydration levels (water fractions lower than about 20%), the segmental dynamics as studied by dielectric techniques is decoupled from the glass transition detected by calorimetry (where it is detected for water fractions equal to or higher than 10%),⁴⁴ as the former probe mainly electrical polarization processes within the water clusters. By this scenario, it is expected that the acceleration and the increase of relaxation strength of the secondary relaxation of polar groups are being gradually saturated, as additional water molecules contribute to a more global movement of the hydrated system, while the extended water clusters are growing in space with the addition of water, leading to the formation of a percolating cluster of the hydration water,⁴⁹ and the subsequent covering of the entire protein surface. The formation of this percolating water cluster is accompanied by the saturation of the relaxation process of water molecules themselves in the uncrystallized phase (ν process).

Regarding the percolation threshold, our measurements suggest that it is reached at water fractions of about 18%. This was verified in more detail in ref 44 by TSDC, at numerous hydration levels in small steps (and in Figure 3 here). This value is also consistent with the hydration range between 13 and 20% where the percolation threshold is detected by dielectric measurements for most globular proteins.⁶¹ In Figure 8, the temperature dependence of the ν relaxation of water for the samples of water fractions above the percolating threshold is shown. The trace is identical for all three samples of 18, 28, and 40% of water. It must be mentioned at this point that the data seem to exhibit a crossover from one Arrhenius behavior at low temperatures to another Arrhenius one at higher temperatures with higher activation energy, at about 170 K. The position of the data correlates well with the thick line in Figure 8, which has been suggested by Ngai et al. in ref 36 to be the trace of the ν relaxation of water. Additionally, the activation energy of these relaxations, which has been calculated taking into account only the points at temperatures lower than the crossover, is in the range of the reported values for the main relaxation of water, at about 0.55 eV (Table 2). The comparison of numerous measurements in various water containing systems (including hydrated BSA) has shown that water exhibits a common dynamic behavior, expressed by the relaxation named ν ,^{34,36}

with a bottom limit of the relaxation times described by the thick line in Figure 8.

The corresponding relaxation strength of the ν relaxation is shown in Figure 9, together with that of the local relaxation of polar groups described earlier. The values of $\Delta\epsilon$ for the sample of 18% in water are in the range of the values obtained for the relaxation of polar groups for a water fraction of 13%, at least in the common temperature range where the two relaxations are observed within the experimental window. This fact supports the assumption that the initial water population, which is involved in the dynamics of the ν relaxation, comes from water molecules interacting with protein polar groups at low hydrations. Further increase of hydration level causes an increase of the dielectric strength, showing that the percolating water cluster, the completion of which is gradually achieved, involves a higher amount of water molecules. At this point, we should highlight the fact that the temperature dependence of $\Delta\epsilon$ of the ν relaxation of water for samples 18 and 28% is characteristic of a secondary relaxation,³⁶ as $\Delta\epsilon$ increases with temperature. Regarding the sample of 40%, a saturation of the dielectric strength of the ν relaxation is observed. This is consistent with the result in ref 44 concerning the fraction of uncrystallized water in BSA–water mixtures calculated by DSC, which showed that it remained stable to about 20% for water fractions higher than about 30%, which is the critical water fraction for crystallization of water during cooling.

Summarizing, considering the interplay between the relaxation of polar groups triggered by water and the ν relaxation of water, we may suggest the following: (i) they are both secondary relaxations, as their relaxation strength increases with temperature, (ii) the water population involved in the relaxation of polar groups is a part of the larger one which is involved in the ν relaxation (comparable dielectric strengths for 13 and 18%, see above), and (iii) the ν relaxation, although it is related to the relaxation of polar groups, is in fact a separate mode of water in the protein hydration shell, activated as soon as water clustering sets in while its relaxation time saturates when the percolating water cluster is formed. This last suggestion is driven by the fact that the ν relaxation is no more plasticized by further addition of water beyond the percolating threshold, as well as by the fact that its magnitude saturates at water fractions where water crystallizes during cooling, where, in parallel, the formation of the primary hydration shell of the protein is completed.^{62,63} In ref 36, the ν relaxation is characterized as a secondary Johari–Golstein (JG) relaxation of water, differing from the JG of simple glass formers, because water molecules can rotate and translate after breaking two hydrogen bonds, like in bulk water.

4.3. Excess Uncrystallized Water and Ice. The temperature dependence of relaxation times for the additional relaxations observed for the samples of water fractions 28 and 40%, that is, for the relaxations attributed to ice and the relaxation named w in Figures 4, 5, and 6, together with the ones for the ν relaxation for the same samples and for the α relaxation from Figure 7a, are plotted in Figure 10, together with experimental data taken from the literature.

In order to assign the rest of the relaxations in Figure 10, we take into account DSC results by ref 44 for the same samples. Particularly, the sample of water fraction 28% is in the hydration range where cold crystallization of water is dominant (at temperatures higher than about 230 K), as crystallization during cooling occurs for water fractions higher than about 30%. The sample of 40% shows crystallization of water during

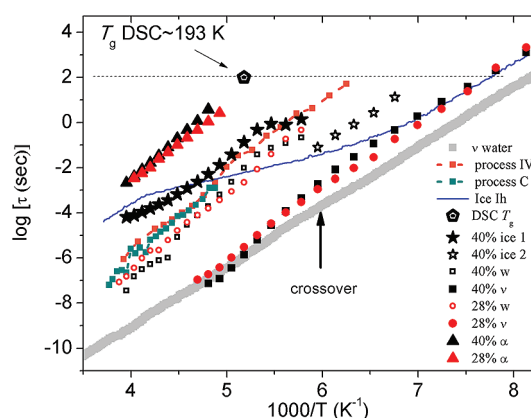


Figure 10. (a) Temperature dependence of the relaxation times for the α relaxation and the relaxations originating mainly from water for a hydrated pellet and a BSA–water solution of water fractions 28 and 40%, respectively, i.e., for the ν relaxation of BSA 28% (red circles) and 40% (black squares), the w relaxation for BSA 28% (open red circles) and BSA 40% (open black squares), and relaxations *ice1* (solid stars) and *ice2* (open stars), for a BSA–water solution of water fraction 40%. The dotted pentagon shows the T_g of hydrated BSA measured by DSC in ref 44 for water fractions higher than 30%. The thick solid line shows a bottom limit for the relaxation times of the ν relaxation of water by ref 36. The blue line shows the dielectric response of Ice Ih by ref 64. Lines and squares correspond to the trace of process C (cyan) and process IV (orange) measured in refs 45 and 42, respectively.

cooling. By these observations, we may conclude that the w relaxation which was detected for both samples of water fractions, 28 and 40%, probably originates from contributions of excess water near the protein surface, in the sense that it is not crystallized during cooling. In the same aspect, the data for relaxation *ice2* and *ice1* in Figure 10 for the sample of water fraction 40% are interpreted as ice contributions, since they do not appear in the spectra of samples with water fraction 28%. Dielectric data of Ice Ih from ref 64 are added to Figure 10 for comparison. The trace of Ice Ih at low temperatures seems to correlate with the one of the ν relaxation, while the data of *ice2*, although they follow a similar slope, they are located at higher temperatures. This fact is not an inconsistency, as it has been shown in the case of various forms of ice (polycrystalline pure ice,⁶⁵ ice microcrystals dispersed in oil,⁶⁶ and frozen aqueous solutions⁶⁷) that the time scale of the relaxation depends on the concentration of defects in the ice crystals and the peak temperature of the relaxation increases with increasing defect concentration. In the high temperature side of Figure 10, the data corresponding to the *ice1* relaxation can be seen. Surprisingly, the temperature dependence of the relaxation times of this relaxation follows a Vogel–Tammann–Fulcher–Hesse dependence, at temperatures higher than about 180 K. A possible scenario explaining the deviation from the Arrhenius behavior can be that relaxation *ice1* describes the motion of structural defects in frozen water clusters of small size, which follow the cooperative movement of the global system. On the other hand, the data of the *ice1* relaxation peak agree very well with the temperature dependence of the time scale of the so-called relaxation of percolating protons observed in hydrated lysozyme which has been assigned to a structural rearrangement of the hydrogen bonding network. This comparison is quite interesting, considering that the protons in hydration water diffuse along the H-bonded network of water molecules

adsorbed on the protein surface in a manner similar to the Grotthuss mechanism for charge transport in ice.⁶⁸ At temperatures lower than 170 K, where the crossover is observed in the case of the ν relaxation, the trace of *ice2* is observed. The relation of the two processes, *ice1* and *ice2*, should be further examined in the future. Anyway, analysis of more measurements at higher water fractions, in combination with measurements on samples of different thermal history, would be essential for better understanding of the dynamics of various water hydrogen bonding networks within proteins.

We turn now our attention to the w relaxation. We recall that the peak of this relaxation could not be clearly discerned in the dielectric loss curves, although it seems that it is essential to fit the data, using a sum of Cole–Cole functions. For that reason, literature data corresponding to relaxations recorded in other hydrated biopolymers are added in Figure 10. A very interesting observation is the fact that the trace of the w relaxation is in quite good accordance to the data for process IV observed in a hydrated myoglobin sample of water fraction 33%, by DRS measurements using insulating thin foils in ref 42, and to process C observed by the same method in a water–glutathione solution of water fraction 20%,⁴⁵ and that in both cases the samples showed no crystallization of water during cooling. These processes in both papers were not assigned to any particulate origin. Nevertheless, their existence supports the validity of the points in this paper for the w relaxation, at least with respect to the relaxation times. The fact that these processes were recorded for samples at intermediate hydration levels, probably in the water fraction region where cold crystallization effects occur, and that they exhibit quite similar temperature dependence of relaxation times, although they are observed in qualitatively different samples, in the sense that hydrated myoglobin in ref 42 was in the form of a hydrated pellet, like in the case of the BSA–water sample of 28% water fraction, while the water–glutathione sample in ref 45 was in a form of a solution and the BSA 40% sample in the form of a concentrated solution, provides additional support on both the existence and the validity of the analysis of the w relaxation. The origin of this process is not clear at this point and could be assigned to the layer of molecules adjacent and strongly interacting with the substrate surface. This is the water layer known to have the highest density and slowest translational dynamics compared to the average.²⁴ Of course, the complexity of the systems studied along with the quality of the results make it difficult to conclude with certainty about the origin of the w relaxation. The possibility that the latter originates to a small amount of “primitive” ice forms or even to protein fluctuations that are enhanced by ice formation (protein cold denaturation) cannot be excluded. The particular relaxation will be further examined in future work.

5. CONCLUSIONS

Water and protein dynamics in hydrated BSA mixtures over wide ranges of composition, in the water fraction range 0–40 wt %, was studied by dielectric relaxation spectroscopy (DRS). Several relaxation processes were identified depending on hydration level:

- (i) The α relaxation associated with the glass transition of the hydrated system was observed by DRS for water fractions equal to or higher than 7%. A strong plasticization by water was observed until a water fraction of 28%. The plasticization stops at higher

water fractions, that is, at water fractions higher than the critical water fraction for crystallization of water during cooling (as measured by calorimetry).⁴⁴

- (ii) The main relaxation of hydration water was followed over the water composition range of the measurements. It was found that, at low water fractions, hydration water triggers a secondary relaxation of small polar groups on the protein surface of an average activation energy value of $E_{\text{act}} = 0.6$ eV, which was detected also for the dry sample. A plasticisation of the relaxation of polar groups was detected until a water fraction of 13%. The dielectric strength of the corresponding relaxation was found to increase in general with water content. At higher water fractions, and, specifically, at water fractions equal or higher than 18%, which corresponds to the water fraction for the formation of a percolating conductive cluster, the position of the ν relaxation of water saturates in the Arrhenius diagram and is described by an Arrhenius law with an activation energy of about 0.55 eV. Additionally, the data imply the existence of a crossover at about 170 K. Its dielectric strength increases initially and then saturates at water fractions higher than 28%. Our results support the claim that the ν relaxation is the secondary Johari–Goldstein relaxation of water, similar to that in bulk water, in the sense that water molecules are able to rotate and translate.³⁶
- (iii) A relaxation denoted as w is observed for water fractions 28 and 40%. It is suggested that this relaxation originates from excess water, in the sense that it does not crystallize during cooling. It has been found that the time scale of the w relaxation is comparable to the traces of two unknown relaxations observed on other hydrated biopolymers.^{42,45}
- (iv) Two dielectric relaxations (at different temperature intervals) attributed to ice-like water structures were detected for the sample of 40%.

From these results, it becomes clear that dielectric studies of protein–water mixtures in wide ranges of composition can be very helpful to clarify the origin of the various relaxations present, when combined with other experimental techniques, e.g., calorimetry. More studies on other globular and fibrous protein–water systems and even higher water fractions may help to clarify the issues raised here. The use of insulating thin foils for better peak resolution but also measurements by different thermal protocols, measurements in progress, will be very helpful to study the effect of crystallization effects to water organization. The use of pressure as an additional parameter could also be highlighting, with respect to the dynamics of water under confinement.

AUTHOR INFORMATION

Corresponding Author

*Phone: +30 210 772 2974. Fax: +30 210 772 2932. E-mail: panagann@mail.ntua.gr.

Notes

The authors declare no competing financial interest.

ACKNOWLEDGMENTS

This research has been cofinanced by the European Union (European Social Fund – ESF) and Greek national funds through the Operational Program “Education and Lifelong Learning” of the National Strategic Reference Framework

(NSRF) - Research Funding Program: Heracleitus II. Investing in knowledge society through the European Social Fund.

REFERENCES

- (1) Mishima, O.; Stanley, H. E. *Nature* **1998**, 396, 329–335.
- (2) Cervený, S.; Colmenero, J.; Alegria, A. *Macromolecules* **2005**, 38, 7056–7063.
- (3) Cervený, S.; Schwartz, G. A.; Alegria, A.; Bergman, R.; Swenson, J. J. *Chem. Phys.* **2006**, 124, 194501–194509.
- (4) Cervený, S.; Alegria, A.; Colmenero, J. *Phys. Rev. E* **2008**, 77, 031803–031807.
- (5) Hayashi, Y.; Puzenko, A.; Feldman, Y. *J. Non-Cryst. Solids* **2006**, 352, 4696–4703.
- (6) Shinyashiki, N.; Shimomura, M.; Ushiyama, T.; Miyagawa, T.; Yagihara, S. *J. Phys. Chem. B* **2007**, 111, 10079–10087.
- (7) Sugimoto, H.; Miki, T.; Kanayama, K.; Norimoto, M. *J. Non-Cryst. Solids* **2008**, 354, 3220–3224.
- (8) Shinyashiki, N.; Yamamoto, W.; Yokoyama, A.; Yoshinari, T.; Yagihara, S.; Ngai, K. L.; Capaccioli, S. *J. Phys. Chem. B* **2009**, 113, 14448–14456.
- (9) Oguni, M.; Maruyama, S.; Wakabayashi, K.; Nagoe, A. *Chem.—Asian J.* **2007**, 2 (4), 514–520.
- (10) Pissis, P.; Laudat, J.; Daoukaki, D.; Kyritsis, A. *J. Non-Cryst. Solids* **1994**, 171, 201–207.
- (11) Bergman, R.; Swenson, J. *Nature* **2000**, 403, 283–286.
- (12) Bergman, R.; Swenson, J.; Börjesson, L.; Jacobsson, P. J. *Chem. Phys.* **2000**, 113, 357–363.
- (13) Ryabov, Y. E.; Puzenko, A.; Feldman, Y. *Phys. Rev. B* **2004**, 69, 014204–014204.
- (14) Ngai, K. L.; Capaccioli, S.; Shinyashiki, N. *J. Phys. Chem. B* **2008**, 112, 3286–3287.
- (15) Capaccioli, S.; Ngai, K. L.; Ancherbak, S.; Rolla, P. A.; Shinyashiki, N. *J. Non-Cryst. Solids* **2010**, 257, 641–654.
- (16) Sjöström, J.; Mattsson, J.; Bergman, R.; Johansson, E.; Josefsson, K.; Svantesson, D.; Swenson, J. *Phys. Chem. Chem. Phys.* **2010**, 12, 10452–10456.
- (17) Cervený, S.; Schwarz, G. A.; Bergman, R.; Swenson, J. *Phys. Rev. Lett.* **2004**, 93, 245702–245704.
- (18) Swenson, J.; Jansson, H.; Bergman, R. *Phys. Rev. Lett.* **2006**, 96, 247802–247805.
- (19) Franzese, G.; Bianco, V.; Iskov, S. *Food Biophys.* **2011**, 6, 186–198.
- (20) Gainaru, C.; Fillmer, A.; Böhmer, R. *J. Phys. Chem. B* **2009**, 113, 12628–12631.
- (21) Khododadadi, S.; Pawlus, S.; Row, J. H.; Garcia Sakai, V.; Mamontov, E.; Sokolov, A. P. *J. Chem. Phys.* **2008**, 128, 195106–195111.
- (22) Doster, W.; Busch, S.; Gaspar, A. M.; Appavou, M.-S.; Wuttke, J.; Scheer, H. *Phys. Rev. Lett.* **2010**, 104, 098101–098104.
- (23) Mazza, G. M.; Stokely, K.; Pagnotta, S. E.; Bruni, F.; Stanley, H. E.; Franzese, G. *Proc. Natl. Acad. Sci. U.S.A.* **2011**, 108, 19873–19878.
- (24) Bruni, F.; Mancinelli, R.; Ricci, M. A. *Phys. Chem. Chem. Phys.* **2011**, 13, 19773–19779.
- (25) Angell, C. A.; Sare, E. J. *J. Chem. Phys.* **1970**, 52, 1058–1068.
- (26) Johari, G. P.; Hallbrucker, A.; Mayer, E. *Nature (London)* **1987**, 330, 552–553.
- (27) Debenedetti, P. G. *Metaestable Liquids*; Princeton University Press: Princeton, NJ, 1996.
- (28) Capaccioli, S.; Ngai, K. L. *J. Chem. Phys.* **2011**, 135, 104504–104512.
- (29) Starr, F. W.; Angell, C. A.; Stanley, H. E. *Phys. A* **2003**, 323, 51–66.
- (30) Velikov, V.; Borick, S.; Angell, C. A. *Science* **2001**, 294, 2335–2338.
- (31) Yu, Y.; Angell, C. A. *Nature* **2004**, 427, 717–720.
- (32) Giovambattista, N.; Angell, C. A.; Sciortino, F.; Stanley, H. E. *Phys. Rev. Lett.* **2004**, 93, 047801–047804.
- (33) Swenson, J.; Teixeira, J. *J. Chem. Phys.* **2010**, 132, 014508–014513.
- (34) Shinyashiki, N.; Sudo, S.; Yagihara, S.; Spanoudaki, A.; Kyritsis, A.; Pissis, P. *J. Phys.: Condens. Matter* **2007**, 19, 205113–205125.
- (35) Capaccioli, S.; Ngai, K. L.; Shinyashiki, N. *J. Phys. Chem. B* **2007**, 111, 8197–8209.
- (36) Ngai, K. L.; Capaccioli, S.; Ancherbak, S.; Shinyashiki, N. *Philos. Mag.* **2011**, 91, 1809–1835.
- (37) Cooke, R.; Kuntz, I. D. *Annu. Rev. Biophys. Bioeng.* **1974**, 3, 95–126.
- (38) Franks, F. *Philos. Trans. R. Soc., B* **1977**, 278, 89–96.
- (39) Harvey, S. C.; Hoekstra, P. J. *J. Phys. Chem.* **1972**, 76, 2987–2994.
- (40) Kimmich, R.; Gneiting, T.; Kotitschke, K.; Schnur, G. *Biophys. J.* **1990**, 58, 1183–1197.
- (41) Kotitschke, K.; Kimmich, R.; Rommel, E.; Parak, F. *Prog. Colloid Polym. Sci.* **1990**, 83, 211–215.
- (42) Jansson, H.; Swenson, J. *Biochim. Biophys. Acta* **2010**, 1804, 20–26.
- (43) Panagopoulou, A.; Kyritsis, A.; Aravantinou, A. M.; Nanopoulos, D.; Sabater i Serra, R.; Gómez Ribellez, J. L.; Shinyashiki, N.; Pissis, P. *Food Biophys.* **2011**, 6, 199–209.
- (44) Panagopoulou, A.; Kyritsis, A.; Sabater i Serra, R.; Gómez Ribellez, J. L.; Shinyashiki, N.; Pissis, P. *Biochim. Biophys. Acta* **2011**, 1814, 1984–1996.
- (45) Pagnotta, S. A.; Cervený, S.; Alegria, A.; Colmenero, J. *Phys. Chem. Chem. Phys.* **2010**, 12, 10512–10517.
- (46) Almutawah, A.; Barker, S. A.; Belton, P. S. *Biomacromolecules* **2007**, 8, 1601–1606.
- (47) Kremer, F.; Schönhals, A. *Broadband Dielectric Spectroscopy*; Springer: Berlin, 2002.
- (48) Cole, R. H.; Cole, K. S. *J. Chem. Phys.* **1942**, 10, 98–105.
- (49) Rupley, J. A.; Careri, G. *Adv. Protein Chem.* **1991**, 41, 37–172.
- (50) Wübberhorst, M.; van Turnhout, J. *J. Non-Cryst. Solids* **2002**, 305, 40–49.
- (51) Gutina, A.; Antropova, T.; Rysakiewicz-Pazec, E.; Virnik, K.; Feldman, Y. *Microporous Mesoporous Mater.* **2003**, 58, 237–254.
- (52) Suherman, P. M.; Taylor, P.; Smith, G. J. *J. Non-Cryst. Solids* **2002**, 305, 317–321.
- (53) Richert, R.; Agapov, A.; Sokolov, A. P. *J. Chem. Phys.* **2011**, 134, 104508–104514.
- (54) Gregory, R. B. *Protein-solvent interactions*; Marcel Dekker: New York, 1995.
- (55) Ringe, D.; Petsko, G. A. *Biophys. Chem.* **2003**, 105, 667–680.
- (56) Fenimore, P. W.; Frauenfelder, H.; McMahon, B. H.; Young, R. D. *Proc. Natl. Acad. Sci. U.S.A.* **2004**, 101, 14408–14413.
- (57) Khododadadi, S.; Malkovskiy, A.; Kisliuk, A.; Sokolov, A. P. *Biochim. Biophys. Acta* **2010**, 1804, 15–19.
- (58) Miyazaki, Y.; Matsuo, T.; Suga, H. *J. Phys. Chem. B* **2000**, 104, 8044–8052.
- (59) Jansson, H.; Bergman, R.; Swenson, J. *J. Phys. Chem. B* **2011**, 115, 4099–4109.
- (60) Anagnostopoulou-Konsta, A.; Pissis, P. *J. Phys. D: Appl. Phys.* **1987**, 20, 1168–1174.
- (61) Careri, G. *Prog. Biophys. Mol. Biol.* **1998**, 70, 223–249.
- (62) Sartor, G.; Hallbrucker, A.; Hofer, K.; Mayer, E. *J. Phys. Chem.* **1992**, 96, 5133–5138.
- (63) Sartor, G.; Hallbrucker, A.; Mayer, E. *Biophys. J.* **1995**, 69, 2679–2694.
- (64) Johari, G. P.; Whalley, E. *J. Chem. Phys.* **1981**, 75, 1333–1340.
- (65) Pissis, P.; Boudouris, G.; Garson, J. C.; Leveque, J. L. *Z. Naturforsch.* **1981**, 36a, 321–328.
- (66) Pissis, P.; Apeki, L.; Christodoulides, C.; Boudouris, G. *Z. Naturforsch.* **1982**, 37a, 1000–1004.
- (67) Daoukaki-Diamanti, D.; Pissis, P.; Boudouris, G. *J. Chem. Phys.* **1984**, 91, 315–325.
- (68) Pagnotta, S. E.; Bruni, F.; Senesi, R.; Pietropaolo, A. *Biophys. J.* **2009**, 96, 1939–1943.